An Enhanced Colour Shift Keying Modulation Scheme for High Speed Wireless Visible Light Communications

R. Singh, *Student Member, IEEE,*, T. O'Farrell, *Member, IEEE,*, and J. P. R. David, *Fellow, IEEE,*

Abstract—This paper presents a new colour shift keying (CSK) modulation format for wireless visible light communication (VLC), based on four colours instead of the three colours used in the existing IEEE 802.15.7 CSK physical layer standard. The new four colour system uses a novel intensity modulation and direct detection approach to realise a four-dimensional signalling scheme which uses the available colour and signal spaces efficiently. The bit error rate evaluation of both the existing and proposed system shows that the new four colour scheme achieves a significant 4.4 dB electrical SNR gain over the three colour scheme for an AWGN channel. The performance of existing and proposed CSK systems is examined over a range of dispersive optical wireless channels including the channel cross-talk and insertion losses, which reveals that the four colour CSK scheme is more power efficient and reliable than the three colour scheme for a particular amount of delay spread that the optical wireless channel may have.

Index Terms—Visible Light Communications, Colour Shift Keying, IEEE 802.15.7, CIE 1931, Chromaticity, Intensity, Bit Error Rate, Maximum Likelihood.

I. INTRODUCTION

VISIBLE light communication (VLC) systems rely upon visible radiations to convey information through a wireless environment. VLC offers unregulated visible spectrum and high data rates [1][2], with highly energy efficient and cost effective system front ends, to the short-range wireless communications [3][4]. As in other optical wireless communication systems such as IR and UV communications [5][6], VLC systems deploy intensity modulation and direct detection (IM/DD). The source in VLC is generally realised by white light emitting diodes (LEDs) and photo-detector(s) are used at the receiver to detect the transmitted signal through wireless channel.

VLC in conjunction with the RF communication offers potential solutions to the issues wireless communication is currently facing. As per CISCO report [7] the data traffic on mobile, wired and Wi-Fi networks is increasing at very rapid rate. On the other hand the spectrum efficiency gains are saturating for the RF networks. This indicates that there could be a significant network capacity shortfall in the very near future. A solution is to make use of unlicensed visible spectrum available for indoor wireless communication. This will not only provide a spectrum relief to the RF network but will also make the mobile communication simpler, more energy efficient, and less prone to interference [8]. The indoor environment also allows wireless VLC to achieve high data rates due to high signal to noise ratio (SNR) (Typically ≥ 60 dB [9]).

There are various research organisations and groups currently working on VLC, such as Visible Light Communications Consortium (VLCC), Japan Electronics and Information Technology Industries Associations (JEITA), Home Gigabit Access (OMEGA) and the task group IEEE 802.15.7. VLC standardisation initiated in 2007, when JEITA issued two standards, CP-1221 and CP-1222. The first IEEE VLC standard, the IEEE 802.15.7, was published in 2011 with various physical layers (PHYs) and medium access control (MAC) layers with data rates ranging from 11.67 kbit/s to 96 Mbit/s incorporating intensity-flicker mitigation and dimming mode [10][11].

This paper details an investigation of the uncoded IEEE 802.15.7 CSK PHY, referred to as the TriLED (TLED) system because it uses three colour LEDs (Trichromatic LEDs) as a source. The issues within the TLED CSK system related to the detection process and symbol mapping have been addressed. A highly novel four colour LEDs based CSK modulation, referred to as QuadLED (QLED) system, is presented which overcomes the issues within the TLED scheme and provides a better performance using the available chromatic (or colour) and the intensity (or signal) spaces [12] efficiently.

Recently, Drost *et al.* [13] and Monteiro *et al.* [14] have presented different constellation designs for the existing TLED CSK to improve colour balancing. The idea of using more than three LEDs in CSK has been introduced by Butala *et al.* [15] to optimise the colour rendering effect, where the use of multiple TLED sets, each capable of generating their own gamut, has been proposed. However, Butala *et al.* [15] suggest that their system will require the receiver to be able to distinguish between the active TLED sets at the transmitter, which can increase the system complexity. On the other hand, our motivation behind the QLED CSK system has been the communications perspective deficiencies of the TLED CSK system. Moreover, this paper details the system model of QLED CSK exploiting maximum likelihood (ML) detection with multilevel constellations and symbol mapping.

The QLED system is similar to the one explained in [15] as it uses multiple sets of TLED systems. However, the constellation design in QLED for each modulation ensures that multiple TLED sets will only generate the part of their gamut which is not overlapped by any other set. A major contribution of this paper is the realisation of a four-dimensional (4-D) constellation of the QLED system by combining four sets of three-dimensional (3-D) constellations. This allows the receiver to treat the instantaneous intensities detected as a point in the 4-D signal space and hence the receiver does not need to differentiate between TLED sets active at the transmitter.

In this paper, the error performances of both the TLED and QLED CSK systems have been compared over an AWGN and representative wireless optical channels with and without the consideration of the cross-talk and insertion losses incurring due to the properties of LEDs, receive filters and PDs. The analysis of system performance reveals that QLED system outperforms TLED system by achieving approximately up to 4.4 dB of SNR gain for the same BER over an AWGN channel. QLED scheme also proves to be the most power efficient and reliable over the dispersive optical wireless channel. As the normalised delay spread of the optical wireless channel is increased, the power savings with uncoded QLED system tends to infinity comparing to the power requirements of uncoded TLED CSK. The simulated error performances are also compared with the analytical approximations for AWGN channel.

The rest of this paper is organised in the following manner. Section II details the background and working of the TLED CSK system along with its performance estimation over an AWGN channel. Section III explains the working of the QLED CSK system and details its error performance over an AWGN channel. Section IV details the performance of TLED and QLED systems over a dispersive optical wireless channel. Finally, section V gives the concluding remarks.

II. BACKGROUND, WORKING AND BER PERFORMANCE OF TLED CSK

A. Basis of CSK

CSK modulates the intensity of the visible light emitted by multicolour LEDs for information transmission. The modulation scheme is based on the x-y colour coordinates, defined by the international commission on illumination in CIE 1931 colour space [16], shown in Fig. 1. The CIE 1931 colour space chromaticity diagram represents all the colours visible to the human eye with their chromaticity values x and y. The colourful region represents the extent or gamut of human vision. The curved edge with wavelengths listed in nanometres is referred to as the monochromatic or spectral locus, and the straight edge, which is the line joining points A and C, is known as the purple line.

As per the standard [10], three different light sources must be used in a system in order to generate a CSK signal [4], such as Blue, Green and Red monochromatic colour LEDs with central wavelengths of points A, B and C, respectively, shown in Fig. 1. The standard have proposed nine valid sets of the three potential sources, to be used in a CSK system, known
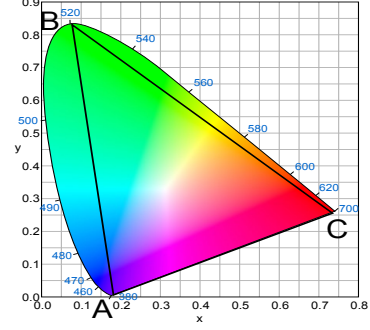

Fig. 1. CIE 1931 colour space chromaticity diagram

as colour band combinations (CBCs) [17]. In TLED CSK, the constellation diagram is of triangular shape, as the triangle ABC shown in Fig. 1. The mixture of light produced from the LED sources allows CSK to regenerate various colours present in the constellation triangle and represent these colours as data symbols.
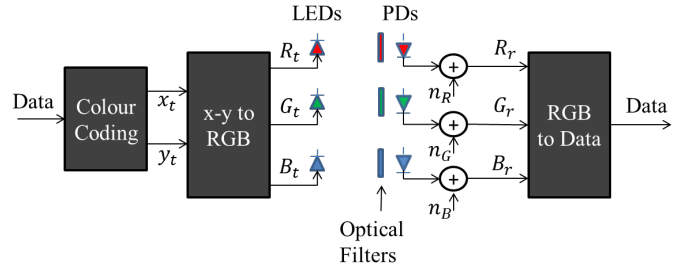
B. TLED CSK System

Fig. 2. Uncoded TLED CSK system

The block diagram of uncoded TLED CSK system is shown in Fig. 2, where x_t, y_t and R_t, G_t, B_t represents the chromaticities and intensities at the transmitter, respectively, and R_r, G_r, B_r are the intensities at the receiver. The independent identically distributed AWGN for each detector is represented by n_R, n_G and n_B. In the TLED system, binary data is first mapped on to x and y chromaticities and these chromaticities are then converted to the intensities P_i, P_j and P_k (or R, G and B) using the following set of equations [10]:

$$x = P_i x_i + P_j x_j + P_k x_k \tag{1}$$

$$y = P_i y_i + P_j y_j + P_k y_k \tag{2}$$

$$P_i + P_j + P_k = 1 \tag{3}$$

In the above set of equations, the (x_i, y_i), (x_j, y_j) and (x_k, y_k) refer to the chromaticity values at the central wavelengths of the three different light sources used in the system. The (x_i, y_i), (x_j, y_j) and (x_k, y_k) also represent one CSK symbol each, with remaining symbols each denoted by a pair of x and y chromaticities. The central wavelength chromaticities only change when a different colour LED is used. At the receiving end the narrowband optical filters pass light of the

desired wavelength to the PDs. The PDs detect incident light intensities and the binary data is retrieved from each set of received intensities (R_r, G_r and B_r).

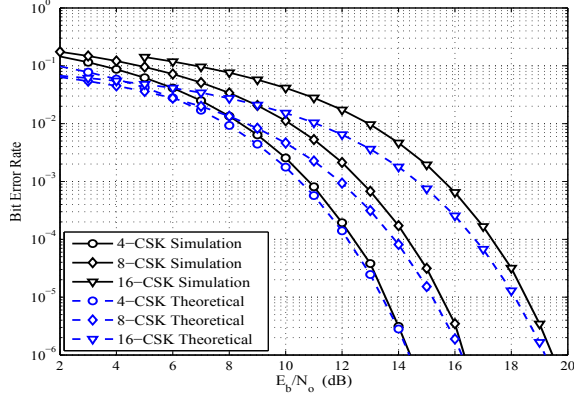### C. Performance over AWGN Channel

Fig. 3. BERs of TLED M-CSK system based on CBC-1 in AWGN on E_b/N_o scale (ML Detection on received intensities)
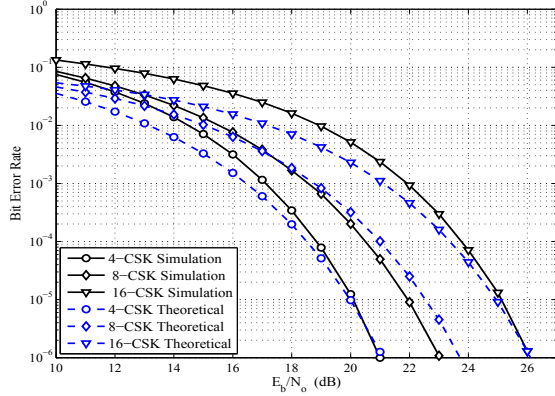

Fig. 4. BERs of TLED M-CSK system based on CBC-1 in AWGN on E_b/N_o scale (Detection on received chromaticities)

As mentioned earlier there are nine valid CBCs for CSK. We have previously investigated these CBCs in [18], where we have evaluated the performance of uncoded IEEE 802.15.7 CSK PHY based on light chromaticity detection as proposed by the standard [10] and other authors in [4][19]. However, Anh and Kwon, have recently explained the colour and signal space for multi-colour LEDs based VLC in [12]. The colour and signal space applies to CSK based systems and therefore, for the TLED CSK systems, symbol detection can take place on the received light intensities as well as the light chromaticity. Throughout this work we focus on the light intensity detection and briefly discuss how chromaticity based detection can lead to poor system performance.

As in [18], we assumed uncoded TLED CSK system and based the performance analysis on CBC-1. Although the error performance of standardised CSK PHY with various CBCs varies [18] when detection takes place in the chromatic space. However, it is not true with detection in the signal space.

This is because the minimum Euclidean distances in the signal space for various constellations of different CBCs are identical, therefore, their performances will be almost the same. Table VI in Appendix E shows the d_{min} for different constellations of all the nine CBCs of CSK.

By defining dispersion free channel conditions and unit responsivity of PDs (i.e. $R = 1$ A/W), the TLED system can be mathematically represented as:

$$\begin{bmatrix} R_r(t) \\ G_r(t) \\ B_r(t) \end{bmatrix} = \begin{bmatrix} R_t(t) \\ G_t(t) \\ B_t(t) \end{bmatrix} + \begin{bmatrix} n_R(t) \\ n_G(t) \\ n_B(t) \end{bmatrix} \quad (4)$$

The AWGN per detector, $n_R(t)$, $n_G(t)$ and $n_B(t)$, each has a noise variance of σ^2:

$$\sigma^2 = \sigma_{Shot}^2 + \sigma_{Thermal}^2 \quad (5)$$

The shot noise variance is given as, $\sigma_{Shot}^2 = 2qR(P_{Signal}(t) + P_{Daylight})B$ and the thermal noise variance is given as $\sigma_{Thermal}^2 = \frac{4k_bTB}{r}$, where q is the charge on electron, R is the responsivity of PD, B is the bandwidth, $P_{Signal}(t)$ is the instantaneous received power, $P_{Daylight}$ is the mean power received from the diffuse sunlight in indoor environment, k_b is the Boltzmann's constant and T is the temperature (kelvins) of the noise equivalent input resistance r. Generally, in an indoor office environment, the illuminance due to the lighting equipment is ~400lux. In addition, there is ~50lux of daylight available at the centre of the office. Therefore, in simulations $P_{Daylight}$ is assumed to be ~11% of the mean value of $P_{Signal}(t)$.

The received TLED CSK symbols, in the form of $R_r(t)$, $G_r(t)$ and $B_r(t)$ represent a point in the three dimensional intensity or signal space. Through the use of minimum Euclidean distance decision rule, the binary data can be decoded from the received intensity based symbols. In this case, the TLED CSK system works equivalent to a three dimensional M-ary system. Fig. 3 shows the simulated and analytical BER performance for TLED scheme over an AWGN channel with detection in the signal space. The calculations for the analytical results have been detailed in Appendix A.

Fig. 4, shows the BER performance of TLED CSK based on chromaticity detection as suggested by the standard [10] and other publications [4],[18],[19]. Clearly, this detection is sub-optimal as the conversion from the intensity to chromaticity causes the noise added to each set of chromaticity co-ordinates to be self correlated. The calculations for the analytical results have been detailed in Appendix A.

D. Gray Mapping in TLED CSK

As the constellation shape in the TLED CSK is triangular, achieving a good 1st and 2nd order Gray mapping is a challenging task. In Appendix B, Fig. 14 shows the symbol mapping for three different modulation sizes in TLED CSK system. For each constellation, all the nearest neighbour symbols have a hamming distance of one, except for (0 1 0) to (1 1 1) in Fig. 14(b) and (1 0 0 0) to (1 1 0 1) in Fig. 14(c). Therefore, the Gray mapping for the TLED system is not robust and must be improved.

III. PROPOSED QLED CSK SYSTEM
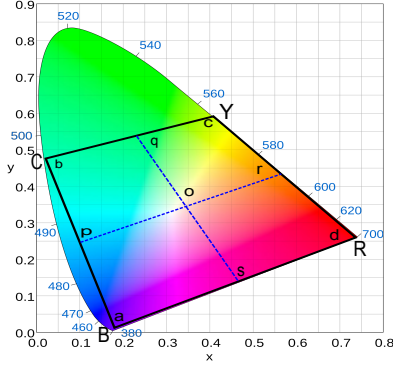
A. Basis of QLED CSK

Fig. 5. Operational colour space of the QLED CSK system on the CIE 1931 x-y colour co-ordinate diagram

The QLED CSK, like TLED CSK is a CIE 1931 colour space based modulation scheme. However, in QLED CSK, the intensity of the light illuminated by four different colour LEDs is modulated. Therefore, QLED CSK is a four dimensional M-ary modulation scheme (considering detection on the light intensity in the signal space). The four different sources are blue, cyan, yellow and red (BCYR) LEDs. The use of BCYR LEDs in CSK forms a quadrilateral constellation shape instead of triangular and allows simple symbol mapping and constellation design as in M-QAM schemes. Fig. 5 shows the operational colour space of the QLED CSK in a quadrilateral region denoted by "abcd" vertices on the CIE 1931 xy colour co-ordinates. Multi-colour LEDs with highly saturated colours are available commercially, by Philips [20], which can be approximately operated at chromaticity points shown by "abcd" vertices in Fig. 5 and can be used for colour mixing.

For the transformation between the intensities and chromaticities, extending the set of linear equations (1-3), to incorporate the light from the fourth LED gives:

$$x = P_i x_i + P_j x_j + P_k x_k + P_l x_l \qquad (6)$$

$$y = P_i y_i + P_j y_j + P_k y_k + P_l y_l \qquad (7)$$

$$P_i + P_j + P_k + P_l = 1 \qquad (8)$$

However, the above set of linear equations (6-8), does not have an accurate solution and gives negative values for intensities, given a set of chromaticities. Therefore, the QLED system had to be designed in such a way that it only uses up to three LEDs at any instance and uses the same equations as the TLED CSK, equations (1-3), for the intensity to chromaticity conversion and vice-versa. This novel QLED system switches between four TLED CSK systems in order to illuminate the colours inside the "abcd" quadrilateral region in Fig. 5. The QLED system requires at least three LEDs to irradiate at specific intensities in order to illuminate any colour present inside the "abcd" quadrilateral, two LEDs for any colour on the border lines and one at the central wavelength position (or at the vertices). The "abcd" quadrilateral is further divided in to four smaller regions. The colours within these small regions

can be illuminated by three LEDs e.g. BCY LEDs for the top left ("pbqo" region), CYR LEDs for the top right ("oqcr" region), YRB LEDs for the bottom right ("sord" region) and RBC LEDs for the bottom left ("apos" region) regions, respectively. Therefore, only up to three out of four LEDs will be "ON" at any time instance in the QLED system and hence, the total optical power used will be equal to the TLED CSK. However, the additional LED means the overall electrical power requirements will increase as the extra LED will need a certain level of biasing due to switching requirements.
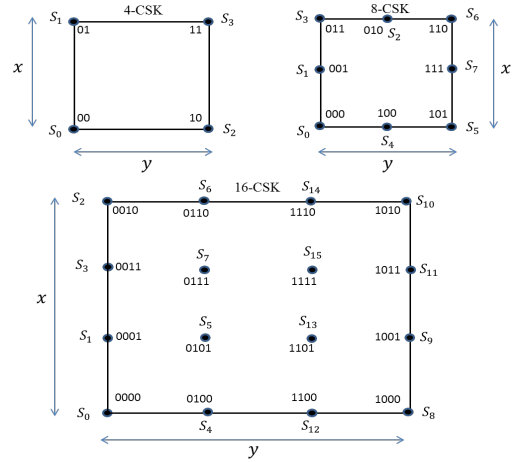

Fig. 6. QLED CSK symbol mapping and symbol point allocation

Fig. 6 shows the symbol mapping and the symbol point allocation design rule for QLED 4, 8 and 16 CSK, in which symbol number along with the assigned data bits are shown. All three constellations are Gray mapped. For 4-CSK and 16-CSK the Gray mapping is same as in [21] for QPSK and 16-QAM, respectively. The symbol mapping for 64-CSK is exactly the same as the 64-QAM modulation, however, not shown in this paper for brevity. In 4-CSK modulation, the symbols are located at the central wavelength chromaticity values (CWCV) of BCYR LEDs. For 8-CSK, symbols S_0, S_3, S_5 and S_6 are located at the CWCVs and symbols S_1, S_2, S_4 and S_7 divide the line connecting CWCVs in equal sections. For 16-CSK and 64-CSK, four symbols are located on the CWCVs, symbols located on the lines joining CWCVs divide the lines into equal parts and the symbols located within the constellation border are approximately at equal distance from their nearest neighbours, as desired.

Table I shows the pair of chromaticities used to represent each QLED CSK symbol for 4-CSK and 8-CSK (see Appendix D for 16-CSK and Appendix C for 64-CSK). Table I also shows the intensities, which can be calculated from chromaticities using equations 1, 2 and 3. It must be noted that the value of central wavelength chromaticities used in equations (1), (2) and (3) varies for different symbols and depends on the symbol position (i.e. the chromaticity value for the symbol) on the "abcd" quadrilateral region in Fig. 5. The intensities used for 64-CSK are not shown in this paper for brevity. As in the TLED CSK, the total optical power transmitted at any instance is constant and equal to one watt in the QLED CSK system i.e. $B + C + Y + R = 1$W, this eliminates any kind of

TABLE I
UNIQUE CHROMATICITY VALUES AND BCYR INTENSITIES FOR
DIFFERENT SYMBOLS OF QLED 4-CSK AND 8-CSK MODULATIONS

	Symbol	x	y	B (w/m^2)	C (w/m^2)	Y (w/m^2)	R (w/m^2)
4-CSK	S_0	0.169	0.007	1	0	0	0
	S_1	0.011	0.460	0	1	0	0
	S_2	0.734	0.265	0	0	0	1
	S_3	0.402	0.597	0	0	1	0
8-CSK	S_0	0.169	0.007	1	0	0	0
	S_1	0.09	0.2335	0.5	0.5	0	0
	S_2	0.2065	0.5285	0	0.5	0.5	0
	S_3	0.011	0.460	0	1	0	0
	S_4	0.4515	0.1360	0.5	0	0	0.5
	S_5	0.734	0.265	0	0	0	1
	S_6	0.402	0.597	0	0	1	0
	S_7	0.568	0.431	0	0	0.5	0.5

Fig. 8. Constellation plot for QLED M-CSK system on a two dimensional chromaticity space

flicker issues related to intensity variations [4]. However, the output power for individual LEDs varies which can be seen from Table I and Table V in Appendix D. On the other hand, the average light chromaticity or colour temperature values can also affect the human circadian rhythm and cognitive functions such as alertness, mood, executive function and memory of humans [22]. For example, under the illumination of an average warm white colour temperature ($\approx 3500K$) humans can feel very relaxed and an average cool white colour temperature ($\approx 17000K$) can oppositely make humans feel very active [23]. The QLED scheme's multilevel constellations have been designed to have an average light chromaticity values around $[x = 1/3, y = 1/3]$, which approximates to a day-light colour temperature of $\approx 6500K$.

Fig. 7 depicts the uncoded QLED CSK system diagram. At the transmitter the data bits are grouped into symbols of k bits and mapped to BCYR intensities required to produce a unique colour which is represented by a pair of chromaticity values. As the conversion from chromaticities to intensities or vice-versa is fixed, it does not have to be repeated at the transmitter or receiver sides. At the receiving side, the optical filters pass light only with desired wavelength to the PDs. The intensities B_r, C_r, Y_r and R_r are then de-mapped back to the data bits via minimum Euclidean distance decision rule.
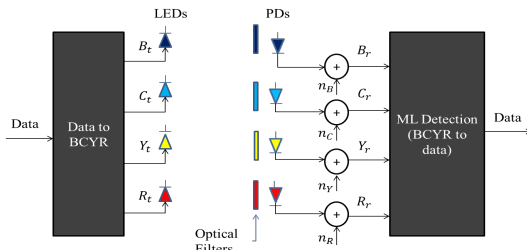

Fig. 7. QLED block diagram in perfect channel conditions without FEC

B. Performance Evaluation of QLED CSK in AWGN

Fig. 8 shows the transmit constellation diagrams for 4, 8, 16 and 64 CSK of the QLED system, on a two dimensional chromaticity space, produced using data given in Tables I, V
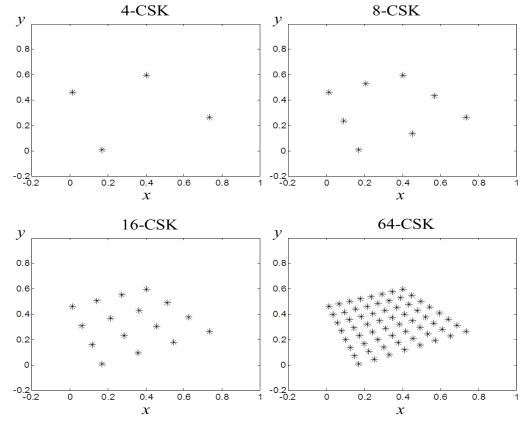
and IV. Fig. 9 shows the BERs for each of the four uncoded QLED CSK modulations over the AWGN channel modelled similarly as in section II-C. A gain of approximately 4 dB can be noted for 4-CSK and 4.4 dB for 16-CSK, and in the case of 8-CSK the gain is roughly 2.9 dB when compared to the results in Fig. 3 of the TLED CSK. In Fig. 9 the analytical error performance of the QLED CSK have also been compared with the simulation results and a good agreement between the two can be observed in the high E_b/N_o region, as expected. The calculations for the analytical results have been detailed in Appendix A. The analytical BER calculation is based only upon the probability of a symbol being received as its nearest neighbour due to AWGN, which is true when either the d_{min} is large or the SNR is high. Therefore, at low SNR or low E_b/N_o, for higher modulation orders such as 16-CSK and 64-CSK where d_{min} is small, there is a disagreement between the analytical and the simulated BER curves.
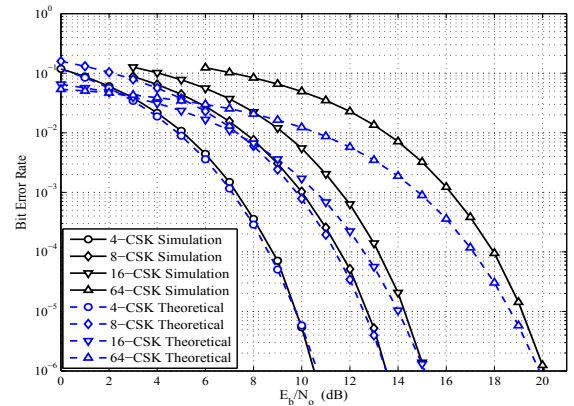
Fig. 9. BERs of QLED M-CSK system in AWGN without FEC, and assuming dispersion-free channel conditions

This high gain of the QLED CSK is mainly due to four dimensional signalling using BCYR LEDs, which increases the Euclidean distance between the symbols when compared to the three dimensional TLED CSK scheme. The four symbols of 4-CSK in the QLED system are orthogonal to each other as can be noted from Table I. As the constellation size increases

above four, the orthogonality in QLED CSK is not held any more. The 1st and 2nd order Gray mapping of symbols is also another advantage of the QLED CSK system. The Euclidean distances between the CSK symbols in the signal space are larger than in the chromatic space, however, the nearest to furthest neighbours of each symbol remain almost the same in both of the spaces. Therefore, the Gray mapping of symbols in the chromatic space works well even when the decision is made in the signal space. In order to check whether the Gray mapping improved the system performance, the QLED CSK system was tested using random symbol mapping for each transmitted symbol. This revealed that the Gray mapping achieves SNR gains up to ~1 dB as the modulation order increases above 4-CSK.

C. Key Observations on the QLED CSK System

The additional LED at the transmitter, PD and a filter at the receiver means the overall system cost could increase by $\approx 33\%$, assuming equivalent unit prices. However, the QLED scheme, when compared to TLED scheme, has an SNR gain of approximately 2.9 to 4.4 dB for the same data rates at a reasonable BER. This SNR gain could be traded by having less number of LED clusters in a QLED scheme. For example, a TLED cluster of 9 LEDs (3 x TLED) could be replaced with an 8 LED cluster of QLED (2 x QLED) for approximately same luminance levels, data rate and performance. This way in fact, the QLED scheme can reduce the overall costs for a CSK system.

At the same time, given a low unit price of these optical front ends, if same number of LED clusters are used for both the TLED and QLED CSK, the QLED scheme will have higher flexibility for the data-rate vs operating range trade-off. For example, comparing the results in Fig. 9 and Fig. 3, we can notice that a 16-CSK QLED system has approximately the same Eb/No requirements as 4-CSK TLED, Hence, QLED CSK will almost double the data-rates for the same indoor SNR.

IV. PERFORMANCE OF TLED AND QLED SYSTEMS OVER DISPERSIVE OPTICAL WIRELESS CHANNEL

In this section, the performance of uncoded, unequalised TLED and QLED CSK systems over a non line-of-sight (LOS), dispersive optical wireless channel is investigated. The non LOS case is used as a worst case scenario where the transmitted visible light signals reflect off multiple room objects and walls, and propagate through various paths with different path lengths towards the receiver. Therefore, only diffuse light signals are present at the receiver. Multiple copies of each transmitted pulse are received by the PDs at different times. The amplitude of these received copies reduce exponentially with time due to the increase in the number of reflections that each path contains. This multipath behaviour of an indoor optical wireless channel causes temporal dispersion of a transmitted optical pulse and inter-symbol interference (ISI) between multiple transmitted data symbols. In a LOS case, assuming minimum cross-talk and no insertion losses, the TLED and QLED systems will perform equivalent to the performance estimations in section II-C and III-B.

A. Optical Channel Model

The indoor dispersive optical channel is generally modelled as an impulse response of a low-pass filter [24],[25]. In this paper, the exponential-decay model has been used to represent the indoor wireless visible light channel, whose impulse response $h(t)$ can be given as [25]:

$$h(t) = \frac{1}{\tau}\exp(\frac{-t}{\tau})u(t) \tag{9}$$

Where $u(t)$ is the unit step function and τ is the exponential decay time constant, which is related to the channel rms delay spread D_{rms} as $D_{rms} = \tau/2$.

For a CSK system, the properties of optical front ends, such as the spectral response of LEDs, the optical gain and response of receive filters, and the responsivity of PDs also affect the overall system performance. For a TLED system, these properties can be represented by a square cross-talk matrix with insertion losses of equation (10), where $g_{i,j}$ represents the optical front end gain between transmit band i and receive band j. Incorporating G and the dispersive optical channel, the overall TLED system can be mathematically represented by equation (11). Similarly, the mathematical representation for the QLED system can be developed.

$$G = \begin{bmatrix} g_{1,1} & g_{1,2} & g_{1,3} \\ g_{2,1} & g_{2,2} & g_{2,3} \\ g_{3,1} & g_{3,2} & g_{3,3} \end{bmatrix} \tag{10}$$

$$\begin{bmatrix} R_r(t) \\ G_r(t) \\ B_r(t) \end{bmatrix} = \begin{bmatrix} g_{1,1} & g_{1,2} & g_{1,3} \\ g_{2,1} & g_{2,2} & g_{2,3} \\ g_{3,1} & g_{3,2} & g_{3,3} \end{bmatrix} \begin{bmatrix} h(t) * R_t(t) \\ h(t) * G_t(t) \\ h(t) * B_t(t) \end{bmatrix} + \begin{bmatrix} n_R(t) \\ n_G(t) \\ n_B(t) \end{bmatrix} \tag{11}$$

B. Simulations

The performance evaluation of the TLED and QLED CSK systems was carried out over the dispersive optical wireless channel for a wide range of the normalised delay spread, D_t. D_t is generally given as, $D_t = D_{rms}/T_b$, where T_b is the bit duration. As the results from previous section shows that the chromaticity detection gives sub-optimal results, for this section, we only consider the detection on the light intensity. A constant value of symbol rate of 24 MHz (Mega symbol per second) was used for both the TLED and QLED CSK schemes, which gives a data rate of up to 96 Mbit/s for the TLED CSK and 144 Mbit/s for QLED CSK. The performance evaluation in this section has been carried out based on two different cases, which are detailed as follows:

1) Case-A: In this case, for a benchmark performance of TLED and QLED schemes, no cross-talk and insertion losses were induced, i.e. G was assumed to be identity matrix. Fig. 10 shows the optical power requirements of the TLED CSK for a BER of 10^{-6} over a scale of D_t. Fig. 10 also shows the normalised optical power requirements of the OOK (On-off Keying) modulation scheme [24],[25], which has been used as a reference. These results reveal that the TLED system shows higher resilience in the dispersive optical channel than OOK.
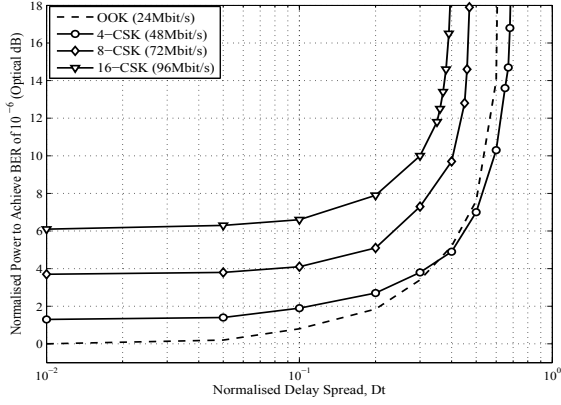
Fig. 10. Dependence of unequalised multipath normalised power requirements on normalised delay spread, for OOK and TLED CSK based on CBC-1, to achieve a BER of 10^{-6}. All the power requirements are relative to the optical power required by OOK in an AWGN channel.

It can be seen from Fig. 10 that 4-CSK has twice the data rate than OOK, however, requires less normalised optical power than OOK for a D_t greater than 0.35. As 8-CSK and 16-CSK offer higher data rates, they require higher optical powers.
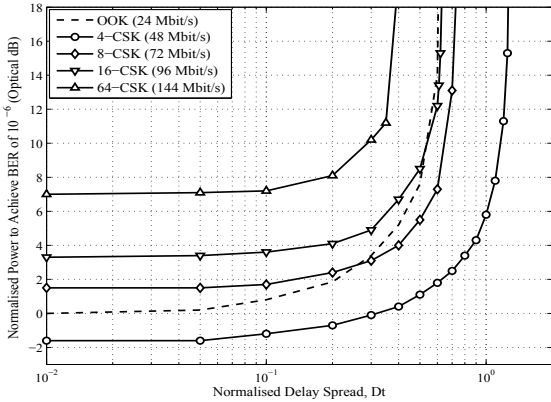

Fig. 11. Dependence of unequalised multipath normalised power requirements on normalised delay spread, for OOK and QLED CSK, to achieve a BER of 10^{-6}. All the power requirements are relative to the optical power required by OOK in an AWGN channel.

Fig. 11 depicts the optical power requirements of the QLED CSK system with respect to D_t. It can be seen from Fig. 11 that 4-CSK modulation of the QLED CSK is the most robust scheme to be used over the dispersive optical channel. Fig. 11 also shows that 8-CSK and 16-CSK modulation schemes of the QLED system also outperform the OOK modulation as the D_t increases. 64-CSK for the QLED system has higher power requirements as it gives higher data rates for the same bandwidth. However, comparing 64-CSK modulation for the QLED system with 16-CSK for the TLED system, it can be found that their power requirements are almost the same as D_t increases. This shows that the QLED CSK is significantly more robust over the dispersive optical channel than the TLED CSK.

2) Case-B: For this case, commercially available optical front-end components were used to estimate the matrix G for both the TLED and QLED schemes. The spectral response of

LED sources [20] LXML-PR01, LXML-PE01, LXM2-PL01 and LXM3-PD01 for QLED, and LXML-PR01, LXM2-PL01 and LXM3-PD01 for the TLED, were used for the evaluation of G. The optical bandpass filters were assumed to be FB450-40 [26], FB500-40 [27], BP590 [28] and FB650-40[29] for QLED, and FB450-40, BP590 and FB650-40 for the TLED CSK. Finally, the spectral response of PC10-6b [?] PD was used.

Fig. 12 shows the optical power requirements of the TLED scheme with the inclusion of channel cross-talk and insertion losses for various levels of D_t. For TLED system, the matrix G was estimated to be:

$$G = \begin{bmatrix} 0.271 & 0.030 & 0 \\ 0 & 0.255 & 0 \\ 0 & 0 & 0.200 \end{bmatrix} \qquad (12)$$

Similarly, Fig. 13 shows the performance of the QLED system produced with following estimation of G:

$$G = \begin{bmatrix} 0.271 & 0.030 & 0 & 0 \\ 0 & 0.255 & 0.002 & 0 \\ 0 & 0.003 & 0.220 & 0.007 \\ 0 & 0 & 0.003 & 0.200 \end{bmatrix} \qquad (13)$$

At the receiver, colour calibration as suggested by the standard [10], was used for TLED and QLED schemes. The colour calibration uses inverse of matrix G, which is multiplied by each set of received symbol in the signal space. Both Fig. 12 and Fig. 13 also show the performance of OOK scheme, which has been produced with the insertion loss due to the responsivity of the PD. The optical filters are not required for OOK.

Fig. 12. Dependence of unequalised multipath normalised power requirements on normalised delay spread including colour cross-talk and insertion losses, for OOK and TLED CSK, to achieve a BER of 10^{-6}. All the power requirements are relative to the optical power required by OOK in an AWGN channel.

C. Analysis of Results

It is clear from results shown in *case-A* and *case-B* that the properties of the optical front-ends leads to higher power requirements for both the TLED and QLED CSK. There is a linear power increment in *case-B* for various levels of D_t. The main reason for this power increment is optical gain of the receive filters and responsivity of the PDs. The channel cross-talk is very small as can be seen from matrices in (12) and (13).

Considering *case-A* and *case-B*, Table II compares the normalised optical power requirements of each modulation
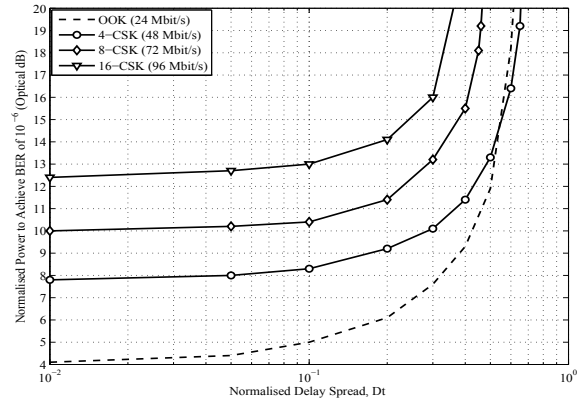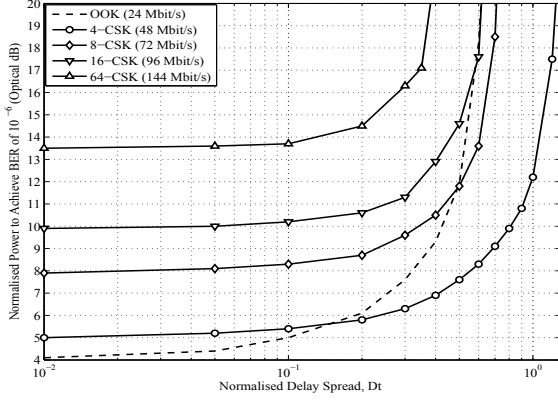
Fig. 13. Dependence of unequalised multipath normalised power requirements on normalised delay spread including colour cross-talk and insertion losses, for OOK and QLED CSK, to achieve a BER of 10^{-6}. All the power requirements are relative to the optical power required by OOK in an AWGN channel.

format of the QLED and TLED CSK for a D_t of 0.3, 0.4 and 0.6. The power requirements of an OOK scheme are also shown. Table II shows that for a higher value of D_t, even though the TLED system based on 4-CSK has a smaller optical power requirements than OOK system, the 8-CSK and 16-CSK modulations will not be able to achieve desired BER performance for a finite amount of power.

At the same time, Table II shows that, for *case-A* and *case-B*, over all the CSK modulation orders, the QLED system is the most power efficient. QLED CSK is also the most robust system to be used over highly dispersive optical channel, such as at D_t of 0.6, where a BER of 10^{-6} can be achieved even at high data rates e.g. 96 Mbit/s (16-CSK).

TABLE II
NORMALISED[1] OPTICAL POWER REQUIREMENTS OF UNCODED AND UNEQUALISED QLED, TLED AND OOK SYSTEMS FOR A BER OF 10^{-6} IN DISPERSIVE OPTICAL CHANNELS

Modulation Scheme			Normalised Optical Power Required for $D_t = 0.3$ (dB)	Normalised Optical Power Required for $D_t = 0.4$ (dB)	Normalised Optical Power Required for $D_t = 0.6$ (dB)
Case-A	QLED	4-CSK	-0.1	0.4	1.8
		8-CSK	3.1	4	7.3
		16-CSK	4.9	6.7	12.2
		64-CSK	10.2	19.9	∞
	TLED	4-CSK	3.8	4.9	10.3
		8-CSK	7.3	9.7	∞
		16-CSK	10	19.9	∞
	OOK		3.4	5.2	14
Case-B	QLED	4-CSK	6.3	6.9	8.3
		8-CSK	9.6	10.5	13.6
		16-CSK	11.3	12.9	17.6
		64-CSK	16.3	21.6	∞
	TLED	4-CSK	10.1	11.4	16.4
		8-CSK	13.2	15.5	∞
		16-CSK	16	22.3	∞
	OOK		7.6	9.3	18.2

[1] Optical Power relative to the Power requirements of OOK in AWGN Channel (dB).

V. CONCLUSION

The standardised TLED CSK system based on CBC-1 of IEEE 802.15.7 has been investigated, and a newly designed QLED CSK system has been presented and recommended over the existing TLED CSK system based on their error performance in an AWGN and dispersive optical wireless channel with and without the inclusion of the cross-talk and insertion losses. The QLED system has enhanced minimum Euclidean distance between the data symbols at the transmitter due to the use of four LEDs and also allows 1st and 2nd order Gray mapping. The performance evaluation shows that, comparing to TLED scheme, QLED scheme has an electrical SNR gain of up to 4.4 dB over AWGN. Over the dispersive optical wireless channels also, the QLED scheme is highly energy efficient and resilient to high level of dispersion when compared to the TLED scheme. The analytical error performance analysis for both of the CSK schemes has also been presented for an AWGN channel.

As a part of future research, the performance evaluation of both the CSK systems with appropriate FEC, interleaving and precoding techniques is sought.

APPENDIX A
THEORETICAL PERFORMANCE OF TLED AND QLED CSK MODULATIONS

As described previously, when the detection takes place on the received intensities, the TLED and QLED CSK systems behave as three and four dimensional M-ary signalling schemes, respectively. Therefore, ML detection can be achieved through a minimum Euclidean distance (d_{min}) rule [30] and the analytical probability of error can be obtained using d_{min} and the number of nearest neighbours, N_n, for each symbol. The symbol error probability based on these parameters can be given as [31]:

$$P_E = \frac{1}{M} \sum_{i=1}^{M} \left\{ N_{ni} Q\left(\sqrt{\frac{d_{min}^2}{2N_0}} \right) \right\} \qquad (14)$$

In the above equation, $Q(.)$ is the tail probability of the standard normal distribution and generally given as

$$Q(x) = \frac{1}{\sqrt{2\pi}} \int_x^\infty e^{-\frac{u^2}{2}} du$$

and N_0 is the one-sided noise power spectral density for the AWGN channel that has standard deviation of noise $\sigma = \sqrt{\frac{N_0}{2}}$. By using the data given in Table III, to obtain the values for N_n and d_{min}, the analytical error probabilities of 4-CSK modulation for the TLED can be calculated as:

$$P_E = 3Q\left(\frac{1}{\sqrt{N_0}} \right) \qquad (15)$$

and the analytical error probabilities of 4-CSK modulation for the QLED can be calculated as:

$$P_E = 0.5Q\left(\frac{0.8157}{\sqrt{2N_0}} \right) + 0.5Q\left(\frac{0.817}{\sqrt{2N_0}} \right) \qquad (16)$$

The bit error probability can be approximated as

$$P_B \approx \frac{P_E}{k}$$

Similarly the analytical BERs for 8, 16 and 64 CSK modulation orders were calculated, and compared against the simulations in Fig. 9 and Fig. 3. The analytical results agree reasonably with the simulations, given the analytical approach is well known to give accurate BER at high SNR.

TABLE III
MINIMUM EUCLIDEAN DISTANCE BETWEEN SYMBOLS OF TLED AND QLED 4-CSK MODULATION SCHEMES IN COLOUR SPACE, GIVEN AS (QLED/TLED)

	S_0	S_1	S_2	S_3
S_0	0/0	$\sqrt{2}/0.8157$	$\sqrt{2}/\sqrt{2}$	$\sqrt{2}/\sqrt{2}$
S_1	$\sqrt{2}/0.8157$	0/0	$\sqrt{2}/0.8170$	$\sqrt{2}/0.8170$
S_2	$\sqrt{2}/\sqrt{2}$	$\sqrt{2}/0.8170$	0/0	$\sqrt{2}/\sqrt{2}$
S_3	$\sqrt{2}/\sqrt{2}$	$\sqrt{2}/0.8170$	$\sqrt{2}/\sqrt{2}$	0/0

In the QLED CSK system, the four symbols of 4-CSK are mutually orthogonal. Therefore, the theoretical bit error probability for the 4-CSK in the QLED system can also be given as [32]:

$$P_B = \frac{M}{2} Q\left(\sqrt{\frac{kE_b}{N_0}}\right) \quad (17)$$

In the above equation, M is the modulation order, k is the number of bits ($k = log_2 M$), E_b is the average energy per bit. As the modulation order is further increased in the four dimensional space for 8, 16 and 64 CSK, the symbols do not hold mutual orthogonality any more.

The analytical BER performance in the case of chromaticity based detection, shown in Fig. 4, has also been estimated based on equation (14). In this case the d_{min} is calculated in the chromatic space and σ has been estimated from the average of the variance of noise added in received x and y values. The variance of noise added to x and y chromaticity values can be given as $x_i{}^2\sigma_R{}^2 + x_j{}^2\sigma_G{}^2 + x_k{}^2\sigma_B{}^2$ and $y_i{}^2\sigma_R{}^2 + y_j{}^2\sigma_G{}^2 + y_k{}^2\sigma_B{}^2$, respectively, where, σ_R, σ_G and σ_B are the standard deviation of noise in PDs used for red, green and blue channels. For example, the analytical error probability for TLED 4-CSK based on CBC-1 can be given as:

$$P_E = 0.5Q\left(\frac{0.3}{2\sigma}\right) + 0.25Q\left(\frac{0.3088}{2\sigma}\right)$$
$$+ 0.25Q\left(\frac{0.3884}{2\sigma}\right) \quad (18)$$

Fig. 4 shows a reasonable agreement between the simulation and theoretical BER curves with a cross-over point for each modulation order.
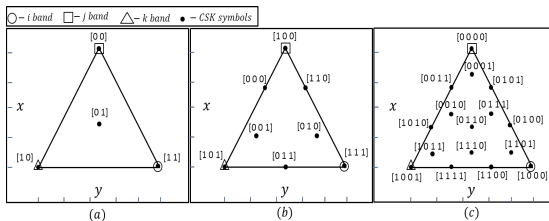
APPENDIX B
SYMBOL MAPPING OF TLED CSK

Fig. 14. TLED M-CSK system's symbol mapping; (a) 4-CSK, (b) 8-CSK, (c) 16-CSK [10]

APPENDIX C
KEY PARAMETERS FOR 64-CSK QLED SYSTEM

TABLE IV
UNIQUE CHROMATICITY VALUES FOR EACH SYMBOL OF QLED 64-CSK MODULATION

Symbol	x	y	Symbol	x	y
S_0	0.1690	0.0070	S_{32}	0.7340	0.2650
S_1	0.1464	0.0717	S_{33}	0.6866	0.3124
S_2	0.1013	0.2011	S_{34}	0.5917	0.4073
S_3	0.1239	0.1364	S_{35}	0.6391	0.3599
S_4	0.0110	0.4600	S_{36}	0.4020	0.5970
S_5	0.0336	0.3953	S_{37}	0.4494	0.5496
S_6	0.0787	0.2659	S_{38}	0.5443	0.4547
S_7	0.0561	0.3306	S_{39}	0.4969	0.5021
S_8	0.2497	0.0439	S_{40}	0.6533	0.2281
S_9	0.2236	0.1061	S_{41}	0.6094	0.2780
S_{10}	0.1714	0.2306	S_{42}	0.5216	0.3778
S_{11}	0.1975	0.1683	S_{43}	0.5655	0.3280
S_{12}	0.0669	0.4796	S_{44}	0.3461	0.5774
S_{13}	0.0930	0.4173	S_{45}	0.3900	0.5297
S_{14}	0.1452	0.2929	S_{46}	0.4778	0.4277
S_{15}	0.1191	0.3551	S_{47}	0.4339	0.4776
S_{16}	0.4111	0.1176	S_{48}	0.4919	0.1544
S_{17}	0.3779	0.1749	S_{49}	0.4551	0.2092
S_{18}	0.3115	0.2895	S_{50}	0.3815	0.3189
S_{19}	0.3447	0.2322	S_{51}	0.4183	0.2641
S_{20}	0.1786	0.5187	S_{52}	0.2344	0.5383
S_{21}	0.2118	0.4614	S_{53}	0.2712	0.4835
S_{22}	0.2782	0.3468	S_{54}	0.3448	0.3738
S_{23}	0.2450	0.4041	S_{55}	0.3080	0.4286
S_{24}	0.3304	0.0807	S_{56}	0.5726	0.1913
S_{25}	0.3007	0.1405	S_{57}	0.5323	0.2436
S_{26}	0.2414	0.2600	S_{58}	0.4516	0.3484
S_{27}	0.2711	0.2003	S_{59}	0.4919	0.2960
S_{28}	0.1227	0.4991	S_{60}	0.2903	0.5579
S_{29}	0.1524	0.4394	S_{61}	0.3306	0.5055
S_{30}	0.2117	0.3198	S_{62}	0.4113	0.4008
S_{31}	0.1820	0.3796	S_{63}	0.3710	0.4531

APPENDIX D
KEY PARAMETERS FOR 16-CSK QLED SYSTEM

TABLE V
UNIQUE CHROMATICITY VALUES AND BCYR INTENSITIES FOR EACH SYMBOL OF QLED 16-CSK MODULATION

Symbol	x	y	B (w/m²)	C (w/m²)	Y (w/m²)	R (w/m²)
S_0	0.1690	0.0070	1	0	0	0
S_1	0.1163	0.1580	0.6667	0.3333	0	0
S_2	0.0110	0.4600	0	1	0	0
S_3	0.0637	0.3090	0.3333	0.6667	0	0
S_4	0.3573	0.0930	0.6667	0	0	0.3333
S_5	0.2853	0.2306	0.3787	0.3247	0	0.2966
S_6	0.1413	0.5057	0	0.6667	0.3333	0
S_7	0.2134	0.3681	0.3202	0.2915	0.3882	0
S_8	0.7340	0.2650	0	0	0	1
S_9	0.6233	0.3757	0	0	0.3333	0.6667
S_{10}	0.4020	0.5970	0	0	1	0
S_{11}	0.5127	0.4863	0	0	0.6667	0.3333
S_{12}	0.5457	0.1790	0.3333	0	0	0.6667
S_{13}	0.4544	0.3031	0.2934	0	0.3428	0.3638
S_{14}	0.2717	0.5513	0	0.3333	0.6667	0
S_{15}	0.3630	0.4272	0	0.3955	0.2563	0.3483

APPENDIX E

TABLE VI
MINIMUM EUCLIDEAN DISTANCE, d_{min}, FOR VARIOUS CBCs OF TLED CSK MEASURED IN WATTS

	Minimum Euclidean Distance (d_{min})		
CBC Number	4-CSK	8-CSK	16-CSK
CBC-1, CBC-3 & CBC-5	0.8157	0.4722	0.2702
CBC-2, CBC-4 & CBC-6	0.8158	0.4708	0.2712
CBC-7	0.8150	0.4719	0.2675
CBC-8	0.8165	0.4701	0.2380
CBC-9	0.8161	0.4701	0.2707

ACKNOWLEDGMENT

REFERENCES

[1] L. Zeng, D. O'Brien, H. Minh, G. Faulkner, K. Lee, D. Jung, Y. Oh, and E. T. Won, "High data rate multiple input multiple output (mimo) optical wireless communications using white led lighting," *Selected Areas in Communications, IEEE Journal on*, vol. 27, no. 9, pp. 1654–1662, 2009.

[2] J. Vucic, C. Kottke, S. Nerreter, K.-D. Langer, and J. Walewski, "513 mbit/s visible light communications link based on dmt-modulation of a white led," *Lightwave Technology, Journal of*, vol. 28, no. 24, pp. 3512–3518, 2010.

[3] D. O"Brien, L. Zeng, H. Le-Minh, G. Faulkner, J. Walewski, and S. Randel, "Visible light communications: Challenges and possibilities," in *Personal, Indoor and Mobile Radio Communications, 2008. PIMRC 2008. IEEE 19th International Symposium on*, 2008, pp. 1–5.

[4] S. Rajagopal, R. Roberts, and S.-K. Lim, "IEEE 802.15.7 visible light communication: modulation schemes and dimming support," *Communications Magazine, IEEE*, vol. 50, no. 3, pp. 72 –82, march 2012.

[5] T. O'Farrell, "Design and evaluation of a high data rate optical wireless system for the diffuse indoor channel using barker spreading codes and rake reception [optical wireless communications]," *Communications, IET*, vol. 2, no. 1, pp. 35–44, 2008.

[6] Z. Xu and B. Sadler, "Ultraviolet communications: Potential and state-of-the-art," *Communications Magazine, IEEE*, vol. 46, no. 5, pp. 67–73, 2008.

[7] C. V. N. I. (VNI), "The zettabyte era [online]. available: http://www.cisco.com," May 2012.

[8] K. Wong, T. O'Farrell, and M. Kiatweerasakul, "The performance of optical wireless ook, 2-ppm and spread spectrum under the effects of multipath dispersion and artificial light interference," *International Journal for Communication Systems*, vol. 13, no. 7-8, pp. 551–576, 2000.

[9] J. Grubor, S. Randel, K.-D. Langer, and J. Walewski, "Bandwidth-efficient indoor optical wireless communications with white light-emitting diodes," in *Communication Systems, Networks and Digital Signal Processing, 2008. CNSDSP 2008. 6th International Symposium on*, 2008, pp. 165–169.

[10] "IEEE Standard for Local and Metropolitan Area Networks–Part 15.7: Short-Range Wireless Optical Communication Using Visible Light," *IEEE Std 802.15.7-2011*, pp. 1 –309, 6 2011.

[11] R. Roberts, S. Rajagopal, and S.-K. Lim, "Ieee 802.15.7 physical layer summary," in *GLOBECOM Workshops (GC Wkshps), 2011 IEEE*, 2011, pp. 772–776.

[12] K.-I. Ahn and J. Kwon, "Color intensity modulation for multicolored visible light communications," *Photonics Technology Letters, IEEE*, vol. 24, no. 24, pp. 2254–2257, 2012.

[13] R. Drost and B. Sadler, "Constellation design for color-shift keying using billiards algorithms," in *GLOBECOM Workshops (GC Wkshps), 2010 IEEE*, 2010, pp. 980–984.

[14] E. Monteiro and S. Hranilovic, "Constellation design for color-shift keying using interior point methods," in *Globecom Workshops (GC Wkshps), 2012 IEEE*, 2012, pp. 1224–1228.

[15] P. Butala, J. Chau, and T. Little, "Metameric modulation for diffuse visible light communications with constant ambient lighting," in *Optical Wireless Communications (IWOW), 2012 International Workshop on*, oct. 2012, pp. 1 –3.

[16] CIE, "Commission Internationale de lEclairage Proc." 1931.

[17] Atsuya Yokoi, Jaeseung Son, Taehan Bae. (2011, march) CSK constellation in all color band combinations. [Online]. Available: http://mentor.ieee.org/802.15/dcn/11/15-11-0247-00-0007-csk-constellation-in-all-color-band-combinations.pdf

[18] R. Singh, T. O'Farrell, and J. David, "Performance Evaluation of IEEE 802.15.7 CSK Physical Layer," in *Globecom Workshops (GC Wkshps), 2013 IEEE, to appear*, Dec 2013.

[19] B. Bai, Q. He, Z. Xu, and Y. Fan, "The color shift key modulation with non-uniform signaling for visible light communication," in *Communications in China Workshops (ICCC), 2012 1st IEEE International Conference on*, 2012, pp. 37–42.

[20] Philips Lumileds, "Luxeon Rebel and Luxeon Rebel ES [Online]. Available: http://www.philipslumileds.com/products/luxeon-rebel/luxeon-rebel-color," 2014.

[21] "Supplement to ieee standard for information technology - telecommunications and information exchange between systems - local and metropolitan area networks - specific requirements. part 11: Wireless lan medium access control (mac) and physical layer (phy) specifications: High-speed physical layer in the 5 ghz band," *IEEE Std 802.11a-1999*, p. i, 1999.

[22] V. B. WJM and V. V. B. GJ, "Lighting for work: a review of visual and biological effects," *Lighting Research and Technology*, vol. 36, pp. 255–269, 2004.

[23] J. Y. Park, R.-Y. Ha, V. Ryu, E. Kim, and Y.-C. Jung, "Effects of color temperature and brightness on electroencephalogram alpha activity in a polychromatic light-emitting diode," *Clin Psychopharmacol Neurosci*, vol. 11, pp. 126–131, 2013.

[24] J. Kahn and J. Barry, "Wireless infrared communications," *Proceedings of the IEEE*, vol. 85, no. 2, pp. 265–298, feb 1997.

[25] J. Carruthers and J. Kahn, "Modeling of nondirected wireless infrared channels," *Communications, IEEE Transactions on*, vol. 45, no. 10, pp. 1260–1268, 1997.

[26] Thorlabs, "FB450-40 Bandpass Filter [Online]. Available: http://www.thorlabs.de/thorproduct.cfm?partnumber=FB450-40," 2014.

[27] ——, "FB500-40 Bandpass Filter [Online]. Available: http://www.thorlabs.de/thorproduct.cfm?partnumber=FB500-40," 2014.

[28] Midopt, "BP590 Bandpass Filter [Online]. Available: http://midopt.com/bp590.html," 2014.

[29] Thorlabs, "FB650-40 Bandpass Filter [Online]. Available: http://www.thorlabs.de/thorproduct.cfm?partnumber=FB650-40," 2014.

[30] John G. Proakis, *Digital Communications*, 3rd ed. McGraw-Hill, 1995.

[31] G. Welti and J. Lee, "Digital transmission with coherent four-dimensional modulation," *Information Theory, IEEE Transactions on*, vol. 20, no. 4, pp. 497–502, 1974.

[32] Bernard Sklar, *Digital Communications: Fundamentals and Applications*, 2nd ed. Prentice-Hall, Inc., 2001.

Ravinder Singh (S'13) graduated with First Class Honours M.Eng degree in Electronic and Communications Engineering from the University of Sheffield, U.K. in 2011. He is currently a PhD student at the same university where he is funded by the department of Electronic and Electrical Engineering. His research involves PHY design for indoor wireless visible light communication.

Timothy O'Farrell (M'91) holds a Chair in Wireless Communication at the University of Sheffield, UK. He is the Academic Coordinator of the MVCE Green Radio Project. His research encompass resource management and physical layer techniques for wireless communication systems. He has led over 18 research projects and published over 200 technical papers including 8 granted patents.

John P. R. David (SM'96–F'12) received the B.Eng. and Ph.D. degrees in electronic engineering from The University of Sheffield, Sheffield, U.K. In 1985, he was with the Central Facility for III-V Semiconductors, Sheffield, where he was involved in the characterization activity. In 2001, he was with Marconi Optical Components (now Bookham Technologies). He is currently a Professor with the Department of Electronic and Electrical Engineering, The University of Sheffield. His current research interests include III-V semiconductor characterization and impact ionization in analog and single photon avalanche photodiodes. Prof. David was an IEEE Lasers and Electro Optics Society Distinguished Lecturer from 2002 to 2004.